The Plant Cell, Vol. 11, 417–430, March 1999, www.plantcell.org © 1999 American Society of Plant Physiologists

Isolation and Characterization of *SYN1*, a *RAD21*-like Gene Essential for Meiosis in Arabidopsis

Xuefang Bai, Brenda N. Peirson, Fugui Dong, Cai Xue, and Christopher A. Makaroff[1]

Department of Chemistry and Biochemistry, Miami University, Oxford, Ohio 45056

The proper pairing, recombination, and segregation of chromosomes are central to meiosis and sexual reproduction. The *syn1* mutation was previously identified as a synaptic mutant in a T-DNA–tagged population of plants. *SYN1* has been isolated and found to exhibit similarity to *Schizosaccharomyces pombe RAD21* and RAD21-like proteins, which are required for chromosome condensation and sister chromatid cohesion during mitosis. Plants homozygous for *syn1* are male and female sterile and show defects in chromosome condensation and pairing beginning at leptonema of meiosis I. Fragmentation of the chromosomes was observed at metaphase I. Alternative promoters produced two *SYN1* transcripts. One transcript was expressed at low levels in most tissues, whereas the other was expressed only in prebolting buds. DNA blot analyses suggest that Arabidopsis contains a small *RAD21* gene family. Consistent with the DNA blot data, a second Arabidopsis *RAD21*-like gene has been identified. These results suggest that different RAD21-like proteins play essential roles in chromosome condensation and pairing during both meiosis and mitosis.

INTRODUCTION

The normal segregation of chromosomes during meiosis in most eukaryotic organisms is dependent on the successful pairing of homologous chromosomes during the zygotene stage of prophase I. After DNA replication, each chromosome enters meiosis as two chromatids. During leptonema of meiotic prophase I, the dispersed chromosomes condense to form long thin threads. During zygonema, homologous chromosomes align, and the synaptonemal complex, an elaborate proteinaceous structure that holds homologs closely apposed along their lengths, is formed. At pachynema, nonsister chromatids of the paired chromosomes recombine, forming chiasmata, which become visible as the chromosomes start to desynapse during diplonema. During meiosis I, sister chromosomes must be attached so that they can orient properly and achieve reductive division. During anaphase I, sister chromosome cohesion is released in preparation for the second meiotic division. Therefore, the formation and proper maintenance of sister chromatid cohesion are essential for the proper alignment and segregation of chromosomes during meiosis (Miyazaki and Orr-Weaver, 1994).

A considerable amount of information is available on the events associated with meiosis in a number of eukaryotic systems, including plants (Dawe, 1998). However, much less is known about the genes required during meiosis in plants than in several other systems, including yeast (Roeder, 1995), Drosophila (Orr-Weaver, 1995), and *Caenorhabditis elegans* (Zetka and Rose, 1995). Based on similarities to meiotic genes identified in other organisms, several genes expressed during meiosis have been identified in Arabidopsis (Sato et al., 1995; Klimyuk and Jones, 1997), lily (Kobayashi et al., 1994), and wheat (Ji and Langridge, 1994). In addition, meiotic mutants have been identified in numerous plants species, including Arabidopsis (Dawson et al., 1993; Chaudhury et al., 1994; He et al., 1996; Peirson et al., 1996; Ross et al., 1997; Spielman et al., 1997; Glover et al., 1998), maize (Golubovskaya et al., 1993, 1997; Maguire et al., 1993; Staiger and Cande, 1993), rice (Kitada and Omura, 1983, 1984), and tomato (Moens, 1969). The characterization of meiotic mutants and their use in the isolation of the corresponding genes are beginning to provide further insight into the molecular events that accompany meiosis in plants.

As part of studies to better understand meiosis in plants, we have characterized a number of T-DNA–tagged male-sterile mutants of Arabidopsis (Peirson et al., 1996). Cytological studies with one mutant line, *syn1*, indicated that it produced polyads containing up to eight microspores with variable amounts of DNA. This suggested that the *syn1* mutation may affect chromosome synapsis and/or recombination. Analysis of chromosomes and microtubules during meiosis revealed that microsporocytes in *syn1* plants contain chromosomes and chromosome fragments that are not attached to microtubule spindles beginning at approximately metaphase I (Peirson et al., 1997). Plants containing the *syn1* mutation are both male and female sterile, indicating that the mutation affects a central aspect of meiosis. Genetic analysis of *syn1* plants indicated that the mutation is

[1] To whom correspondence should be addressed. E-mail makaroca@muohio.edu; fax 513-529-5715.

recessive and tightly linked with the T-DNA insert (Peirson et al., 1996). To understand the role of the SYN1 protein during meiosis and to elucidate better the process of chromosome synapsis and recombination in general, we have cloned and characterized the *SYN1* gene. Results are presented showing that SYN1 is a RAD21-like protein and that it is involved in chromosome condensation and pairing during meiosis.

RESULTS

Cytological Analysis of *syn1* Plants

The effect of the *syn1* mutation on meiosis was analyzed using laser scanning confocal microscopy. The results of the analysis of chromosomes and microtubules in microsporocytes during various stages of meiosis in wild-type plants and mutants are shown in Figure 1. The first detectable defect in *syn1* plants is irregular chromosome condensation during prophase I. Typically, chromosome condensation in wild-type plants is uniform throughout the cell (Figure 1A); regions of highly condensed and dispersed DNA are rarely observed in the same cell. In contrast, chromosome condensation in *syn1* plants is always accompanied by the presence of both regions of highly condensed and highly dispersed chromatin (Figure 1B). Five bivalents were observed that aligned at the equator during metaphase in wild-type plants (Figure 1C). In the mutant, numerous chromosome fragments were observed (Figure 1D). Most of the DNA is present near the metaphase plate in *syn1* plants, suggesting that pairing has occurred. However, univalents and chromosome fragments also are found in the peripheral cytoplasm. Analysis of cells at anaphase I (data not shown) and telophase II (Figure 1F) identified between 26 and 40 chromosome fragments of varying sizes per cell. Based on the number and distribution of these DNA-staining fragments, we conclude that the defect results in fragmentation of the chromosomes. The spindles in *syn1* plants also are not as tightly focused as those observed in wild-type plants (Figure 1E); however, we believe that this is a result of the dispersed nature of the chromosomes and not alterations in the spindle. Nucleation of microtubule filaments on univalents and chromosome fragments is detected often in the peripheral cytoplasm.

To gain further insight into the exact nature of the *syn1* alterations and when they first occur, we analyzed prophase spreads. As shown in Figure 2, the first identifiable defect in *syn1* plants was observed during early leptonema. During leptonema in wild-type microsporocytes, chromosomes appear as long thin threads that loop out of a dense synizetic knot (Figure 2A). In contrast, in *syn1* plants, the synizetic knot always appears more darkly stained, and chromosomes are not observed as thin threads (Figure 2G). During later stages of leptonema in the mutant, the synizetic knot

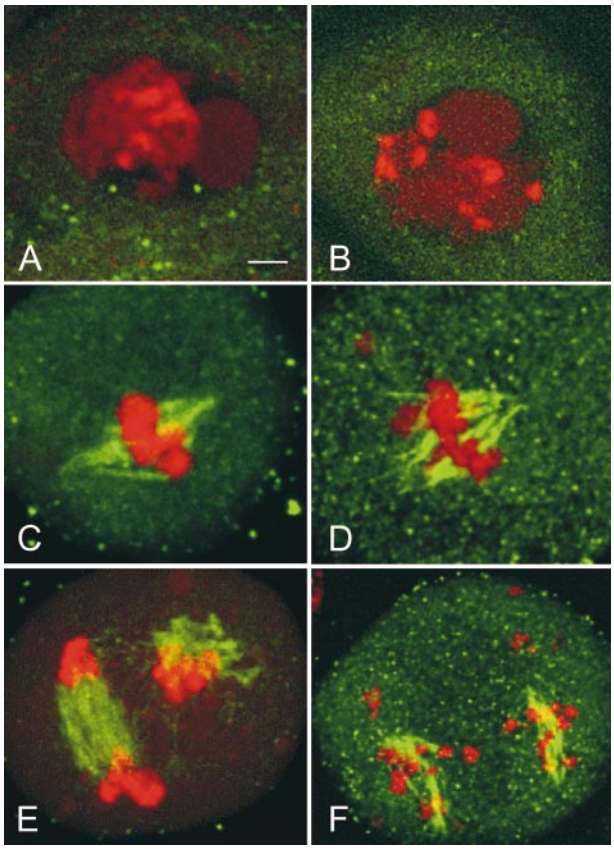

Figure 1. Analysis of Meiosis in Wild-Type and *syn1* Plants by Using Confocal Microscopy.

Chromosomes and microtubules were detected with propidium iodide (red) and anti–β-tubulin antibody in conjunction with fluorescein isothiocyanate–labeled secondary antibody (green). Images were viewed and captured with a Nikon PCM2000 confocal microscope system.

(A) Wild-type microsporocyte at prophase I with condensing chromatin.

(B) *syn1* microsporocyte at prophase I with highly condensed and dispersed chromatin.

(C) Wild-type microsporocyte at metaphase I. Short spindle fibers extend from aligned chromosomes to the two poles.

(D) *syn1* microsporocyte at metaphase I. Most of the chromosomes, which appear fragmented, are gathered at the equator. Chromosome fragments also are observed in the cytoplasm.

(E) Wild-type microsporocyte at telophase II. One spindle is shown parallel to the plane of focus. The second spindle is shown perpendicular to the plane of focus.

(F) *syn1* microsporocyte at telophase II. Chromosome fragments are scattered throughout the cytoplasm. Spindles are parallel to each other.

Bar in **(A)** = 2 μm for **(A)** to **(F)**.

disperses, but the chromatin retains its darkly staining appearance. Normally, chromosome pairing occurs during zygonema, with paired chromosomes readily apparent throughout the cell (Figures 2B and 2C). However, beginning at approximately zygonema in the mutant, a series of intertwined knots was observed. As condensation and pairing continued, the intertwined appearance of the chromosomes worsened (Figure 2H). Chromosomes rarely appeared as thin, threadlike structures in the mutant, and paired chromosomes in a bouquet structure were never observed. Condensation of bivalents occurs during pachynema in normal cells (Figure 2D). In wild-type plants, five bivalents are readily apparent during diplonema and diakinesis (Figures 2E and 2F). In contrast, at approximately diplonema/diakinesis in *syn1* plants, the chromosomes appeared as one mass of condensed chromatin (Figure 2I). Univalents and chromosome fragments typically were not observed before anaphase I. However, on one occasion, a cell at premetaphase I with univalents was observed (Figure 2J). In this cell, ~15 apparent univalents and chromosome fragments can be identified. Typically, at anaphase I in *syn1* cells in which the chromosomes have not been spread during slide preparation, approximately five "chromatids" were observed at the poles, with a considerable number of chromosome fragments remaining at the equator (Figure 2K). In contrast, no less than 25 chromosomes and chromosome fragments were detected in anaphase I cells that have been spread (Figure 2L).

Our observations suggest that although some pairing occurs, complete synapsis of the chromosomes is blocked in *syn1* plants. It appears that the chromosomes are generally intertwined and nonspecifically associated with one another. Therefore, the *syn1* mutation results in defects in both chromosome condensation and pairing, which ultimately results in chromosome fragmentation.

Isolation of the *SYN1* Gene

In previous studies, we demonstrated that there is only one T-DNA insert in *syn1* plants and that it shows tight genetic linkage with the sterility phenotype (Peirson et al., 1996). The kanamycin resistance gene and *syn1* showed consistent cosegregation over several generations of lines either backcrossed to the wild type or allowed to self. In addition, the same T-DNA hybridization pattern was found in DNA gel blots of >50 sterile plants from segregating T_3, T_4, and T_5 families (data not shown). Hybridization patterns predicted that the insert consists of one intact copy of T-DNA flanked by a partial T-DNA copy orientated as an inverted repeat around the right border. Two T-DNA left border plant junction fragments of ~14 and 15 kb were observed when DNA gel blots containing SalI-digested *syn1* DNA were probed with T-DNA left border sequences (data not shown).

To isolate the *SYN1* gene, we conducted left border plasmid rescue experiments and produced a clone that contained 7 kb of plant DNA. Results from DNA gel blot analysis, using the fragment against *syn1* and wild-type plants, confirmed that it did in fact correspond to one of the T-DNA left border plant junctions (data not shown). The plant DNA was subcloned, partially sequenced, and used to screen wild-type λ genomic and cDNA libraries. No significant open reading frames or similarity to known genes were identified in the sequence. To characterize the insertion site more fully, two wild-type λ genomic clones, each containing ~15-kb inserts and corresponding to the insertion site, were obtained.

The DNA sequence of a 7.0-kb region of wild-type DNA around the insertion site was determined. Additional sequence around the *SYN1* locus on chromosome 5 was obtained when the DNA sequence of a P1 clone (MOP10) was submitted to GenBank as accession number AB005241. Analysis of the DNA sequence around the T-DNA insertion site identified two long open reading frames of 598 and 171 codons, ~2.0 and 3.5 kb on either side of the T-DNA insert, respectively. A map of the *SYN1* locus is shown in Figure 3A. The longest open reading frame shows similarity to a glycoamidase gene recently identified in *Aspergillus tubigensis* (Ftouhi-Paquin et al., 1997), whereas the shorter open reading frame shows limited sequence similarity to proline-rich proteins (PRPs) and extensins. Screening of cDNA libraries identified a number of clones for the *PRP*-like gene. Transcripts for this gene are not present in buds (see below). No significant open reading frames or similarity to known sequences were detected in the region immediately flanking the T-DNA insert. However, analysis of the DNA sequence for potential exons with NetPlantGene (Hebsgaard et al., 1996) did identify a number of putative exons.

To determine whether any of the potential exons correspond to the *SYN1* gene, we conducted a series of reverse transcription–polymerase chain reaction (RT-PCR) experiments with poly(A) RNA purified from buds harvested from prebolting plants (buds < 5 mm). We had previously shown that buds <5 mm are enriched in microsporocytes undergoing meiosis (Peirson et al., 1997). RT-PCR experiments using primers specific to several of the predicted exons demonstrated that the predicted exons do in fact correspond to a gene and that the gene is expressed at very low levels. Typically, two rounds of PCR were required to obtain strong amplification products. Additional RT-PCR, inverse PCR (IPCR), and rapid amplification of cDNA ends (RACE) experiments were then conducted to isolate a full-length *SYN1* cDNA. Details of the RT-PCR experiments are presented in Methods. The positions of the primers used in these experiments are shown in Figure 3B. The 5′ and 3′ most primers that allowed amplification of *SYN1* transcripts were primers BP2 and PA3, respectively. A total of 21 exons (Figure 3B, exons A and 1 to 20), corresponding to a 2093-nucleotide transcript, were isolated using the gene-specific primers. The longest exon in the gene is ~200 bp long, whereas the shortest exon is only 21 bp. The *SYN1* gene spans ~5.0 kb. The T-DNA insertion site is located in the middle of intron 8 (Figure 3B).

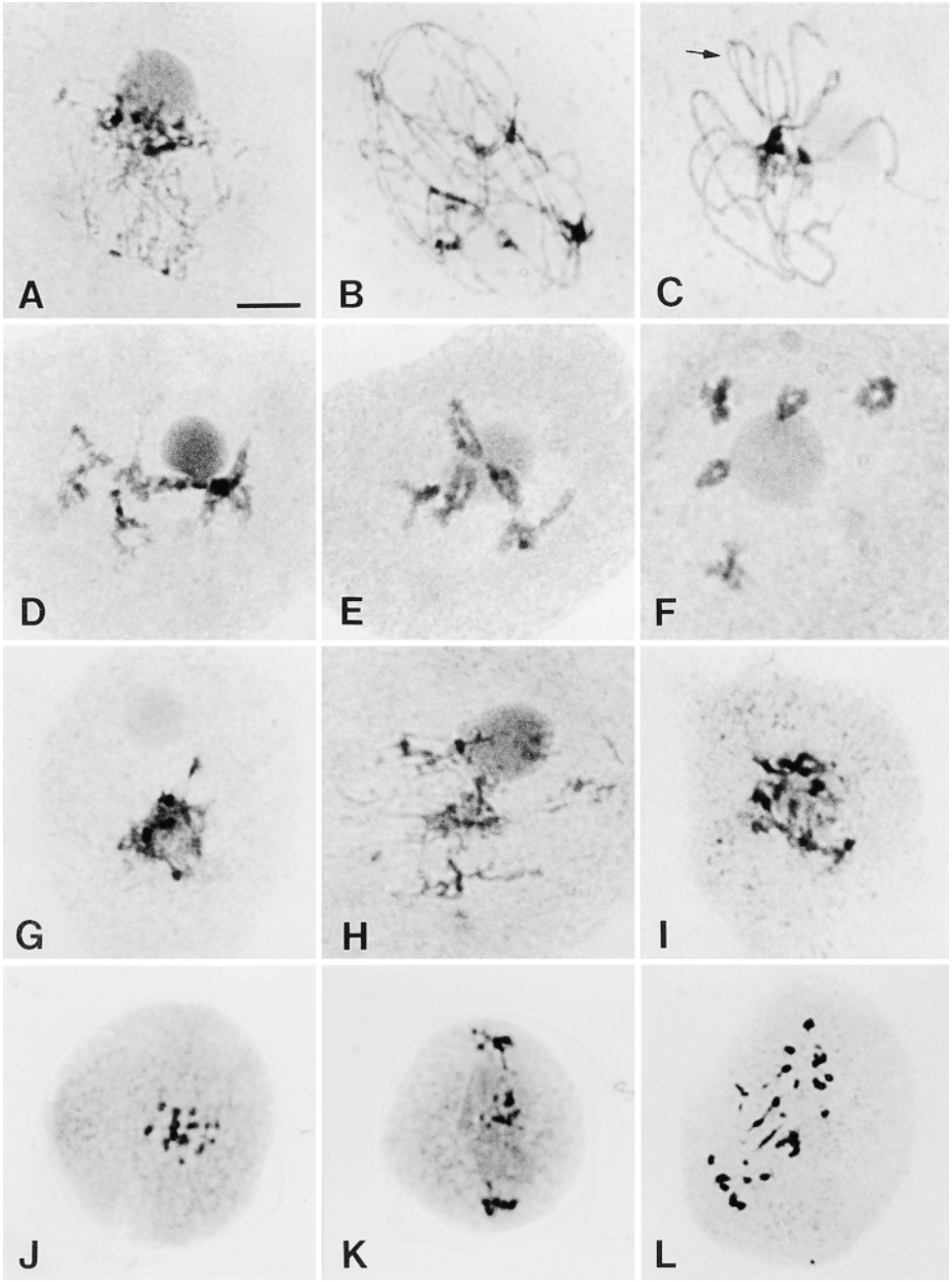

Figure 2. Prophase Spreads of Wild-Type and *syn1* Chromosomes.

Wild-type (**[A]** to **[F]**) and *syn1* (**[G]** to **[L]**) microsporocytes are shown at various stages of meiosis.
(A) Leptonema; chromatin is visible as thin threads.
(B) Early zygonema; chromosomes begin to pair.
(C) Late zygonema; pairing is complete. Chromosomes exhibit classical bouquet structure. Arrow shows an unpaired loop.
(D) Pachynema; condensation of bivalents occurs.
(E) Diplonema; homologs separate but remain attached at chiasmata. Five bivalents are readily observed.
(F) Diakinesis; chromosomes complete condensation. Terminalization of chiasma occurs.
(G) Early leptonema; chromosome condensation begins with the appearance of granular structures.
(H) Zygonema; chromosomes are tangled and have an irregular appearance. Little to no pairing is detectable.
(I) Post-zygonema; chromatin continues to condense as one tangled mass. Individual bivalents are not detectable.

The *SYN1* cDNA sequence obtained from these experiments along with its predicted protein sequence are shown in Figure 4. Analysis of the cDNA, designated as the BP2 transcript, predicted that it has the potential to encode a 627–amino acid protein. In-frame stop codons are present both 5′ and 3′ to the predicted open reading frame. This observation, in conjunction with RT-PCR experiments showing that primers 5′ to BP2 and 3′ to PA3 fail to generate amplification products when used in combination with primers internal to the cloned cDNA (data not shown), indicates that all of the *SYN1* exons have been identified.

To confirm that we do in fact have a full-length cDNA and to map more accurately the 5′ end of the transcript, IPCR was conducted with cDNA generated by reverse transcription with primer BP4. After second-strand synthesis and self-ligation, PCR was conducted with the primer set BP7 and BF67 followed by primer set BP7 and XB4. When the PCR products were cloned and sequenced, they were found to contain exons 1 to 9, as expected. However, instead of containing exon A (shown underlined in Figure 4) spliced to exon 1, as predicted, the IPCR products contained sequences immediately 5′ to exon 1. This sequence (shown as exon B and in boldface in Figures 3B and 4, respectively) forms one continuous exon with exon 1. RT-PCR experiments using primers BP5 and BP6 confirmed that this second form of the transcript, referred to as the BP5 transcript, is real and not an artifact. Therefore, two forms of the *SYN1* transcript, which differ at their 5′ ends, are present in Arabidopsis.

To map the 5′ end of the BP2 transcript, we conducted IPCR experiments using primer XB7, which is specific for exon A of the BP2 transcript, and primer BP7. Analysis of the BP7 and XB7 IPCR products confirmed that the BP2 transcript contains exon A spliced with exons 1 to 9. However, the 5′ most cDNA end obtained in these experiments maps ~80 bp 3′ to the BP2 primer in exon A. Attempts to use 5′ RACE and different IPCR conditions and primers failed to generate longer cDNA clones. However, all of the IPCR clones obtained did map 5′ to the first in-frame methionine in the transcript. Our ability to obtain RT-PCR clones by using the BP2 primer indicates that the *SYN1* transcript must start at or before this position. Therefore, the 5′ end of the BP2 primer is being used to denote the 5′ most end of the BP2 transcript. Difficulties in obtaining cDNA beyond this point may be the result of a short transcript half-life or the high GC content and strong secondary structure that are present in the region, features that have been shown to cause premature termination of reverse transcription in other systems (Green and Sargan, 1991).

The cDNA cloning and IPCR results indicate that (1) T-DNA insertion occurred in the middle of the *SYN1* transcriptional unit and (2) *SYN1* utilizes alternative promoters and splicing patterns to produce two transcripts that differ in their 5′ ends. One transcript (BP2) contains 21 exons, A and 1 to 20, and encodes a 627–amino acid protein, whereas the other (BP5) begins within the first intron of the BP2 transcript, contains 20 exons, and encodes a 617–amino acid protein. No differences in structure or DNA sequence were identified between the BP2 and BP5 transcripts after exon 1, suggesting that they are both derived from *SYN1.* Confirmation of this fact was obtained by RT-PCR experiments. Primer sets BP2/BP6 and BP5/BP6 both failed to amplify *SYN1* sequences from bud RNA isolated from *syn1* plants. By contrast, the expected amplification products were obtained for both primer sets from wild-type RNA. Control RT-PCR experiments using primers for an unrelated gene, *GLX2-2*, showed that the *syn1* RNA preparation was good (data not shown).

Because of the proximity of the glycoamidase-like open reading frame to the 5′ end of the *SYN1* transcript, RACE was conducted to map the 5′ end of the glycoamidase mRNA. In contrast to the difficulties encountered mapping the 5′ end of the *SYN1* transcript, the 5′ end of the glycoamidase-like gene was readily mapped. The longest and most abundant RACE clone obtained maps 50 bp 5′ to the first in-frame methionine. This position maps to the same region as the 5′ most end of the BP2 transcript and in fact overlaps it by 9 bp. The overlapping nature of the transcripts for the two genes is highly unusual and indicates that the regulatory sequences for the genes are found within the coding region of the adjacent gene or within the respective genes.

Analysis of the SYN1 Protein

The polypeptide encoded by the BP2 transcript has a predicted molecular mass of 71,233 D, whereas the predicted protein encoded by the BP5 transcript has a predicted molecular mass of 70,259 D. Overall, the proteins are relatively hydrophilic, containing large numbers of polar (27%) and

Figure 2. (continued).

(J) Premetaphase I; ~15 univalents and chromosome fragments can be seen at the middle of the cell.

(K) Anaphase I; variable numbers of chromatids move to the poles. DNA also remains at the equator. In contrast to the cells shown in the rest of Figure 2, this cell was not squashed. Additional chromosomes and chromosome fragments that are present out of the plane of focus are not visible.

(L) Anaphase I; >25 chromosomes and chromosome fragments are detectable in the cytoplasm.

Bar in **(A)** = 7.5 μm for **(A)** to **(L)**.

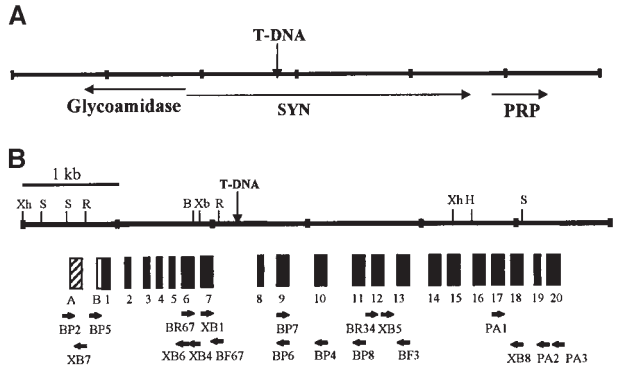

Figure 3. Map of the *SYN1* Locus and Exon Patterns.

(A) Map of a 10-kb region of chromosome 5 showing the relative positions of the genes for SYN1, a glycoamidase-like protein, and a PRP relative to the T-DNA insertion site. Arrows indicate the direction and extent of transcription. The map is marked in 2-kb intervals. **(B)** Partial restriction map of *SYN1.* Restriction sites shown are B, BamHI; H, HindIII; R, EcoRI; S, SacI; Xb, XbaI; and Xh, XhoI. The positions of exons are shown below the map. Exons common to both the BP2 and BP5 transcripts (1 through 20) are shown in black. Exon A, which is present only in the BP2 transcript, is shaded in diagonal stripes. Exon B, which is present only in the BP5 transcript and is located in the first intron of the BP2 transcript, is shown in white. The positions and directions of primers used in this study are shown as horizontal arrows. The map is marked in 1-kb intervals.

charged (32%) amino acids. Comparison of the predicted SYN1 amino acid sequences with sequences in GenBank using a BLAST search (Altschul et al., 1990) indicated that they are similar to the RAD21-like family of proteins. SYN1 is most similar (18% identity) to the frog RAD21 homolog, XRAD21 (Losada et al., 1998). The SYN1 protein encoded by the BP5 transcript is shown aligned with RAD21-like proteins from *C. elegans* (accession number U40029), humans (McKay et al., 1996), *Schizosaccharomyces pombe* (Birkenbihl and Subramani, 1992), frog (Losada et al., 1998), and *Saccharomyces cerevisiae* (Guacci et al., 1997) in Figure 5. The RAD21-like proteins show the greatest sequence conservation at their N and C termini, which are the least hydrophilic regions of the proteins. The N-terminal 90 amino acids of the proteins exhibit the greatest similarity, ranging from 43 to 90% identity. All of the RAD21 homologs, with the exception of yeast MCD1 and the protein encoded by the BP2 transcript, begin with the sequence Met-Phe-Tyr-Ser/Ala (Figure 5). The first 16 amino acids of the protein encoded by the BP2 transcript are different from those encoded by BP5 transcript, including a 10–amino acid extension. The MCD1 protein also contains additional N-terminal residues relative to the other proteins.

The central portions of all the proteins exhibit the least sequence conservation. However, they do share several common features. (1) The central region of all the RAD21-like proteins is hydrophilic and relatively acidic in nature, which is consistent with a potential role in chromatin binding. (2) Signals for nuclear localization are found in the central portions of all the proteins. Analysis of SYN1 with the PSORT program (Horton and Nakai, 1996) identified potential nuclear localization signals at positions 271 (PQPAKKRAR) and 481 (PNRKKRPN). The RAD21 proteins are required early in prophase before the breakdown of the nuclear membrane. (3) All of the proteins contain a PEST sequence, which acts as a signal for rapid protein destruction via the ubiquitin–26S protease or the 26S protease pathways. Many short-lived proteins are known to contain PEST sequences (Rechsteiner and Rogers, 1996). The presence of several PEST sequences in SYN1 suggests that it is probably a short-lived protein, which is consistent with its proposed transient role during meiosis.

Expression Studies

To examine the expression patterns of *SYN1* and the neighboring genes, we used fragments corresponding to the two open reading frames and the *SYN1* cDNA as probes in RNA gel blots. When *SYN1* cDNA sequences were used to probe RNA gel blots of total RNA from roots, leaves, and buds, no signal was detected (data not shown). However, Figure 6A shows that a very low abundance, 2100–nucleotide transcript was detected in poly(A) RNA isolated from prebolting buds. The transcript size corresponds well with the size of the *SYN1* cDNA. *SYN1* transcripts were not detected in poly(A) RNA from seedlings (Figure 6A), suggesting that *SYN1* may be expressed only in reproductive tissue. To test this possibility more rigorously, we conducted PCR with equal amounts of cDNA prepared from prebolting buds and seedlings by using primers that amplify the 3′ end of the gene. Figure 6B shows that although *SYN1* sequences are dramatically higher in the bud cDNA preparation, a low level of amplification product also was obtained from seedlings. These results are similar to those obtained for the Arabidopsis meiotic gene, *AtDMC1*, in which low-level expression was detected in both reproductive and vegetative tissue by using RT-PCR (Klimyuk and Jones, 1997).

To determine whether differences in expression patterns of the two *SYN1* transcripts could be detected, we conducted PCR using either primer BP2 or BP5 in conjunction with primer BF67, which is common to both transcripts. Figure 6B shows that primers BP2 and BF67 produce amplification products in all three tissues of approximately equal intensity. In contrast, primers BP5 and BF67 only produce an amplification product in cDNA prepared from buds. Taken together, these results along with those from earlier PCR experiments suggest that the BP2 transcript is expressed at low levels throughout most of the plant, whereas expression of the BP5 transcript is confined to buds.

Finally, as part of our analysis of the *SYN1* locus, the expression patterns of the glycoamidase- and *PRP*-like genes

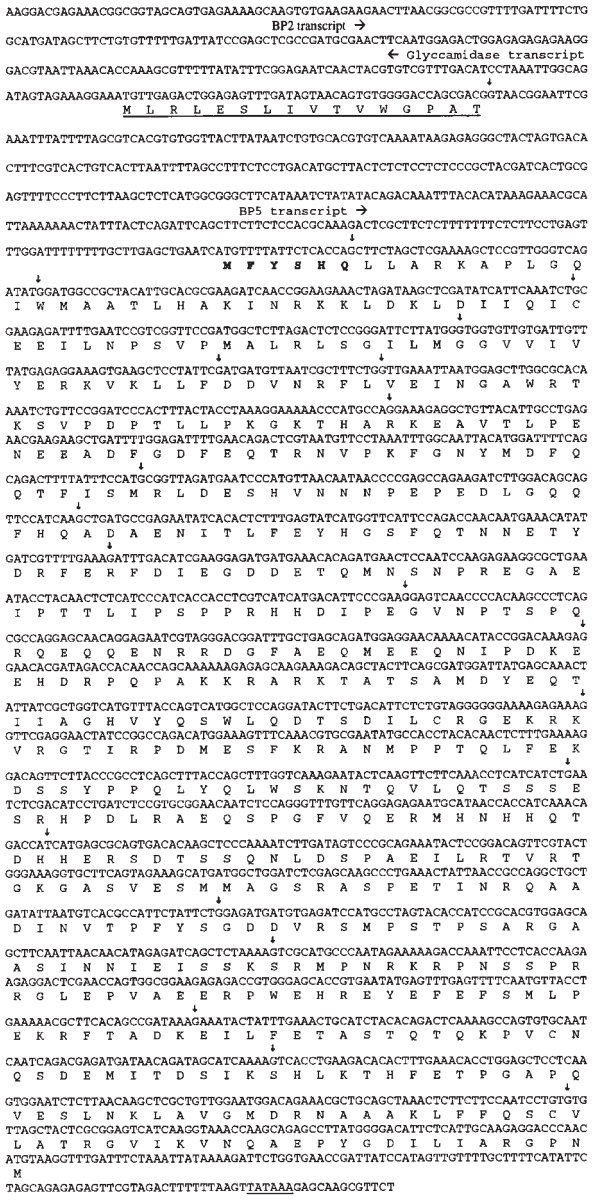

Figure 4. *SYN1* cDNA and Deduced Amino Acid Sequence.

The deduced SYN1 amino acid sequence is shown below the cDNA sequence and a portion of the 5′ flanking sequence. The 5′ ends of the BP2 and BP5 transcripts are shown as horizontal arrows above the sequence. The BP2 transcript encodes a 627–amino acid polypeptide that contains 16 amino acids from exon A (shown underlined) linked with exons 1 to 20. The BP5 transcript encodes a 617–amino acid polypeptide. It begins within intron 1 of the BP2 transcript with exon B (shown in boldface) and includes exons 1 to 20. The position of the 5′ end of the glycoamidase transcript is shown as a horizontal arrow below the sequence. The positions of introns are shown as vertical arrows. A potential polyadenylation signal is underlined. The cDNA sequences for the BP2 and BP5 transcripts have GenBank accession numbers AFO80619 and AFO80620, respectively.

also were evaluated using RNA gel blot analysis. The glycoamidase-like gene is expressed in several tissues. A 2000-nucleotide transcript corresponding to the glycoamidase was detected in total RNA isolated from buds, leaves, and roots (data not shown). Expression of the *PRP*-like gene is more limited. Although a transcript of ~1000 nucleotides was relatively abundant in total RNA from roots and etiolated seedlings, it was not detected in RNA from leaves or buds (data not shown). Therefore, the mRNA for the glycoamidase appears to be constitutively expressed, whereas the expression of the *PRP* gene is more limited.

A *RAD21*-like Gene Family Is Present in Arabidopsis

To determine whether there are other *RAD21*-like homologs in Arabidopsis, we conducted low-stringency DNA gel blot hybridization experiments. Figure 7 shows that sequences corresponding to the first 200 amino acids of the *SYN1* cDNA detect several bands in Arabidopsis genomic DNA. The strongest signal corresponds to the *SYN1* locus. Five to six additional *SYN1* hybridizing fragments were detected in DNA digested with four different restriction enzymes, indicating that sequences similar to *SYN1* are present in the Arabidopsis genome. This result was confirmed by searching the Arabidopsis database. A second *RAD21*-like gene is present on chromosome 5. It maps to the P1 clone MHK7 (GenBank accession number AB011477). Experiments to isolate cDNAs for this second *RAD21* homolog are currently under way. Based on predicted exon sequences for this second *RAD21* gene, the two Arabidopsis RAD21-like proteins are ~16% identical. As expected, the greatest similarity between the proteins is found in the first 90 amino acids (F. Dong and C.A. Makaroff, unpublished data). Therefore, there are at least two *RAD21*-like genes in Arabidopsis. *SYN1* is essential for chromosome condensation and pairing during meiosis. We predict that the second *RAD21*-like gene may be required for proper chromosome condensation and pairing during mitosis.

DISCUSSION

As part of studies to understand better the process of meiosis in plants, we have characterized a T-DNA–tagged, meiotic mutant of Arabidopsis. Cytological analyses of *syn1* plants indicate that the mutation results in defects in chromosome condensation and pairing during the leptotene and early zygotene stages of prophase I. Characterization of the *SYN1* gene indicates that it is a *RAD21* homolog. *RAD21* was first isolated from *S. pombe* as an essential gene involved in DNA double-strand break repair during mitotic growth (Birkenbihl and Subramani, 1992). *S. pombe* RAD21 is a nuclear, cell cycle–regulated phosphoprotein. The phosphorylated form of the protein appears important for protein

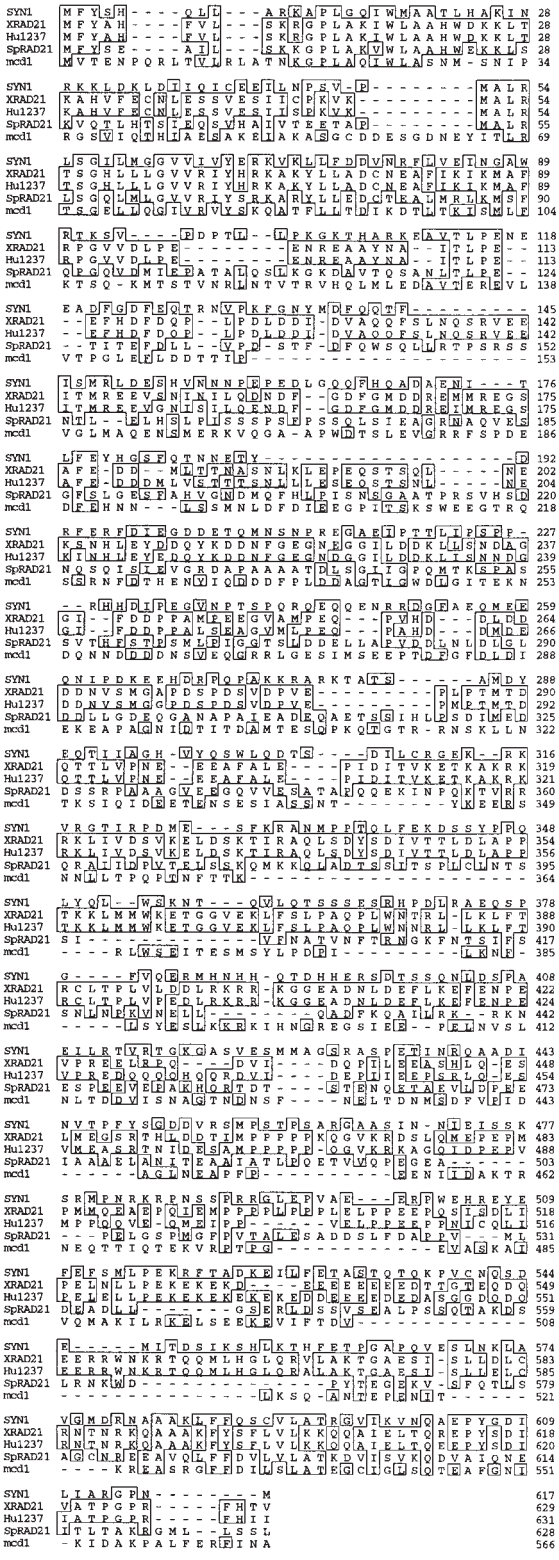

Figure 5. Alignment of RAD21-like Proteins.

The deduced SYN1 amino acid sequence encoded by the BP5 transcript is shown aligned with the sequences of RAD21-like proteins from frog (XRAD21; Losada et al., 1998), humans (Hu1237; McKay et al., 1996), *Schizosaccharomyces pombe* (SpRAD21; Birkenbihl and Subramani, 1992), and *Saccharomyces cerevisiae* (mcd1; Guacci et al., 1997). Sequences were aligned using the Clustal method with a PAM250 residue weight table (Higgins and Sharp, 1989). Residues present at the same position in two or more sequences are boxed. Gaps are shown as dashes.

function in mitosis and cell survival after ionizing radiation (Birkenbihl and Subramani, 1992). Recently, *RAD21* homologs have been isolated from several organisms, including *S. cerevisiae* (Guacci et al., 1997), *C. elegans*, frog (Losada et al., 1998), mouse (Yu et al., 1995), and humans (McKay et al., 1996).

Studies with an *S. cerevisiae RAD21* homolog, referred to as MCD1 (Guacci et al., 1997), SCC1 (Michaelis et al., 1997), and RHC21 (Heo et al., 1998), indicate that it is a cohesin protein that is required for both chromosome condensation and sister chromatid cohesion during mitosis. For simplicity, we refer to the *S. cerevisiae* gene as *MCD1.* Blocks in chromosome condensation and premature sister chromatid separation are observed in *mcd1* temperature-sensitive mutants (Guacci et al., 1997; Michaelis et al., 1997). Like its *S. pombe* homolog, *S. cerevisiae* MCD1 is expressed in a cell cycle–dependent fashion, with transcripts and protein present from S phase to anaphase (Guacci et al., 1997; Michaelis et al., 1997). The MCD1 protein colocalizes with chromatin from early S phase to the time of sister chromatid separation at anaphase (Michaelis et al., 1997). Based on these observations, it was suggested that MCD is a component of the mitotic chromatin condensation machinery in *S. cerevisiae* (Guacci et al., 1997). *mcd1* mutants are sensitive to UV and γ radiation and to the microtubule destabilizing agent nocodazole (Heo et al., 1998). Because of this, it has been proposed that MCD1 also may play a role in (1) the regulation of microtubule function, (2) spindle assembly checkpoint, or (3) the anaphase-promoting complex (Heo et al., 1998).

A second *RAD21*-like gene, *REC8*, also is present in *S. pombe.* In contrast to *RAD21*, *REC8* is expressed only during meiosis (Lin et al., 1992). *rec8* mutations result in impaired meiotic chromosome pairing, alterations in linear element structures, and premature separation of sister chromatids (Molnar et al., 1995). Therefore, it appears that *REC8* is the meiotic counterpart of *RAD21* in *S. pombe.* Budding yeast also contains a second protein, SCU31900, that is similar to RAD21, although its function has yet to be confirmed.

Much less is known about the function of RAD21 proteins in higher eukaryotes. Based on expression patterns, it has been suggested that a mouse RAD21 homolog, mHR21, may be involved in V(D)J and meiotic recombination (McKay

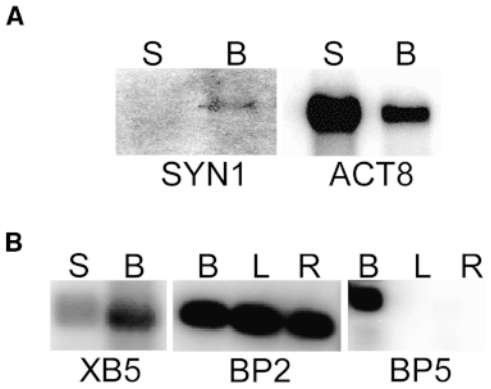

Figure 6. Expression Analysis of the *SYN1* Locus.

(A) RNA gel blot analysis of *SYN1* transcripts. Poly(A) RNA (3 μg) isolated from prebolting buds (B) or seedlings (S) was probed with ^{32}P-labeled PCR fragments for *SYN1* (XB5/XB8) or *ACT8* (An et al., 1996).

(B) PCR analysis of *SYN1* expression. Reverse transcription was conducted with total RNA (4 μg) from seedlings (S), buds (B), leaves (L), and roots (R) by using primer BF67 (for amplifications using primers BP2 or BP5 as the 5′ primer) or primer XB8 (for amplification with XB5 as the 5′ primer). Asymmetric PCR then was conducted using either primer XB5, BP2, or BP5. The products were then used as templates for amplification with primer pairs XB5 and XB8, BP2 and XB4, or BP5 and XB4, which are specific for both *SYN1* transcripts, only the BP2 transcript, or only the BP5 transcript, respectively. The PCR products were separated on a 2.0% agarose gel, transferred to nylon membranes, and probed with cDNA fragments corresponding to each of the amplification products. Amplificaton sets are labeled with the 5′ primer used in the amplification reaction.

et al., 1996). Although *mHR21* transcripts are present at high levels in all tissues, the highest transcript levels are found in the thymus and testis. Like our observations for *SYN1*, two different *mHR21* transcripts were detected. However, the relationship between the two different transcripts has not been determined. A frog RAD21-like protein, XRAD21, which appears to be required for mitotic chromosome cohesion, also has been identified (Losada et al., 1998).

Based on our results for SYN1 and previous data on RAD21-like proteins, it is now clear that members of the RAD21 family of proteins are involved in the formation and maintenance of chromosome cohesion during both mitosis and meiosis. However, questions concerning their specific role(s) in the cell and how they function still exist. For instance, it has been proposed that yeast MCD1 functions as a linker molecule that connects the condensation and cohesion machinery on mitotic chromosomes (Guacci et al., 1997). In contrast, frog XRAD21 is thought to participate only in the cohesion process after condensation has occurred (Losada et al., 1998). Cells immunodepleted for XRAD21 during interphase exhibit defects in chromosome pairing and sister chromatid cohesion that result in the appearance of double-strand breaks; however, chromosome condensation did not appear to be affected. Like MCD1, SYN1 appears to play a role in both the condensation and pairing processes.

Exactly how SYN1 facilitates chromosome condensation and pairing remains to be determined. It is possible that SYN1 is associated with early recombination nodules, small proteinaceous particles that associate with the synaptonemal complex during zygonema. It is thought that early recombination nodules play a role in the presynaptic alignment of chromosomes (Stack et al., 1993). Data from several sources suggest that early recombination nodules, and possibly their associated fibers, play a contractile role by pulling chromosomes from presynaptically aligned distances (2 to 3 μm) to those required for synaptonemal complex formation (0.3 μm) (reviewed in Dawe, 1998). However, alterations are detected in *syn1* plants well before the presynaptic alignment of chromosomes. At the beginning of leptonema in *syn1* plants, the initial condensation of chromosomes is accompanied by the appearance of darkly staining granular structures (Figure 2G). Soon after, a series of intertwined

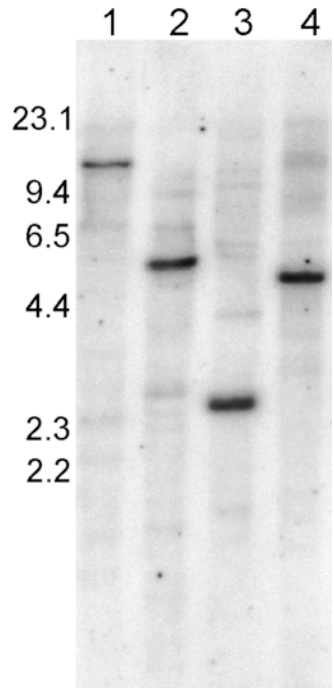

Figure 7. DNA Gel Blot Showing the Presence of *SYN1* Sequences in Arabidopsis.

Total Arabidopsis DNA was digested with PstI (lane 1), HindIII (lane 2), BamHI (lane 3), or SacI (lane 4) and subjected to DNA gel blot analysis using a ^{32}P-labeled PCR fragment generated by amplification of the BP5 cDNA with primers BP5 and XB4. Marker lengths are indicated at left in kilobases.

chromosome knots is observed. Paired or aligned chromosomes are not apparent in *syn1* plants. In contrast, during leptonema in wild-type microsporocytes, chromosomes condense and are visible as long thin threads, which loop out from the synizetic knot (Figure 2A). Aligned (Figure 2B) and paired (Figure 2C) chromosomes are readily apparent in wild-type microsporocytes during zygonema and early pachynema.

Defects in condensation and pairing also affect later aspects of prophase in *syn1* microsporocytes. Cells exhibiting chromosome morphology typical of pachynema, diplonema, and diakinesis are never observed in *syn1* plants. The tangled nature of the chromosomes makes distinguishing individual bivalents and/or univalents very difficult. However, on one occasion, a premetaphase I cell with ~15 univalents and chromosome fragments was observed (Figure 2J). This suggests that pairing did not occur and that the univalents aligned at metaphase I in an "autooriented" configuration. In contrast, the finding of anaphase I cells with five chromatids at the poles (Figure 2K) suggests that some bivalents are formed and align on the spindle. Analysis of optical sections of *syn1* cells at metaphase I suggests that typically a small number of univalents and bivalents actually align on the spindle and that because of the tangled nature of the chromosomes, most of the remaining DNA is pulled to the equator (data not shown). The tangled nature of the chromosomes was best observed at anaphase I. In cells in which the chromosomes have not been spread, five chromatids often can be observed at the poles (Figure 2K). In contrast, when chromosome spreads are prepared and observed, >25 chromosomes and chromosome fragments are found spread throughout the cell. This result indicates that (1) the chromosomes are loosely associated and (2) the chromosomes are fragmented and not just unpaired.

The *syn1*-conferred phenotype is different from that usually found in asynaptic mutants (Singh, 1993), in which univalents are observed at diakinesis, with little to no fragmentation of the chromosomes. In contrast, a normal complement of univalents, which is 10 for Arabidopsis, is never observed at diakinesis in *syn1* plants. The *afd* mutation of maize, which eliminates prophase I (Golubovskaya and Mashenkov, 1975), is most similar to *syn1.* At approximately diakinesis in *afd* plants, ~20 univalents are observed, which align during metaphase I. At anaphase I, the sister chromatids move to opposite poles and 20 chromosomes can be observed at each pole, suggesting that the univalents behave like bivalents. More than 10 apparent univalents have been detected at premetaphase I in *syn1* plants (Figure 2J); however, this is not typical. Rather, the chromosomes typically align at the equator as a tangled mixture of bivalents, univalents, and chromosome fragments. Therefore, although the two mutations share some similarities, they are not identical.

The *syn1* mutation also shows some similarity to the chromosome stickiness (*st*) mutation in maize (Beadle, 1932). In male- and female-sterile plants homozygous for *st*, chromosomes are clumped at prophase I and often tangled. Chromosomal fragmentation is common at anaphase I in *st* plants. Intertwined chromosomes and chromosome fragments are common during meiosis in *syn1* plants. However, in contrast to *syn1*, *st* also causes defects during mitosis. An Arabidopsis meiotic mutant (*mcd1*; Ross et al., 1997) also has been identified that shows a similar but not identical phenotype to *syn1.* Chromosome fragmentation, beginning at approximately diplonema, is observed in *mcd1* plants. However, unlike *syn1*, the *mcd1* mutation confers reduced fertility and not total sterility (Ross et al., 1997).

The chromosome fragmentation observed in *syn1* plants could result from several sources, including strand breakage due to tension on the chromosomes and unrepaired double-strand breaks formed during recombination. At this time, we cannot distinguish between these two possibilities. The tangled appearance of the chromosomes and the apparent lack of chromosome pairing suggest that strand breakage may be occurring. In addition, although it is generally accepted that double-strand break formation precedes synapsis in yeast (Hawley and Arbel, 1993), it is not known whether this is also true for plants. In yeast, a model has been proposed in which single-stranded DNA, generated by double-strand break formation, participates in the homology search required for synapsis and synaptonemal complex formation (Roeder, 1995; Kleckner, 1996). Consistent with this, two RecA-like proteins, DMC1 (Bishop et al., 1992) and RAD51 (Ogawa, 1993), which are involved in recombination, form multiple nuclear complexes on chromosomes before synapsis in yeast (Bishop, 1994). There is also some preliminary evidence that early recombination nodules may participate in the homology search and initiation of synapsis in plants (Albini and Jones, 1987; Stack et al., 1993). RAD51 and LIM15, a DMC1 homolog, also are present at early recombination nodules in lily (Terasawa et al., 1995; Anderson et al., 1997). Therefore, the possibility also exists that the chromosome fragmentation observed in *syn1* microsporocytes could be due to unrepaired double-stranded breaks formed during leptonema.

Our results indicate that two *SYN1* transcripts are produced that differ in their first exons. Whereas the two transcripts are essentially the same size, the first exon of the BP2 transcript is not present in the BP5 mRNA, which begins within intron 1 of the BP2 transcript. Therefore, the SYN1 protein expressed from the BP2 transcript does not contain several highly conserved residues found at the N terminus of most RAD21-like proteins. Analysis of *SYN1* transcript patterns indicates that the BP2 transcript is produced in buds, leaves, and roots, whereas the BP5 transcript is detected only in buds (Figure 6B). This finding, together with the observation that *SYN1* transcripts in general are most abundant in prebolting buds, suggests that the BP2 transcript is produced at low levels in most tissues and that the BP5 transcript is expressed at somewhat higher levels only in buds, presumably during meiosis. The theory that the BP5 transcript represents most of the *SYN1* mRNA in buds is consistent with the fact that only BP5 transcripts

were recovered in IPCR experiments on bud RNA by using primers common to both transcripts.

The finding that *SYN1* BP2 transcripts are found at low levels throughout the plant raises the question of its potential role in processes other than meiosis. Except for the alterations identified in meiosis, no other defect has been detected. Specifically, alterations have not been identified during mitosis in *syn1* plants. It is possible that the BP2-encoded protein has a minor role in mitosis, and its absence does not produce an observable effect. Or, if the BP2-encoded protein does have an essential role, then a second RAD21-like protein may compensate for its absence. Our finding of a second RAD21 homolog on chromosome 5 in Arabidopsis is consistent with this second possibility. The characterization of this second *RAD21*-like locus is not complete. Therefore, we cannot conclude with certainty that it is involved in mitosis. It is clear, however, that it cannot substitute for SYN1 in meiosis.

The observation that the 5′ end of the *SYN1* BP2 transcript overlaps the 5′ terminus of the neighboring glycoamidase gene by at least 9 bp raises interesting questions concerning the regulation of their expression. Given the overlapping nature of the *SYN1* and glycoamidase transcripts, *SYN1* promoter sequences should lie either within the *SYN1* or glycoamidase transcriptional units. To our knowledge, this is a novel observation of overlapping transcripts in plants. Sieburth and Meyerowitz (1997) have shown that the AGAMOUS control region includes sequences both 5′ to and within the gene. Therefore, it is possible that the *SYN1* control region includes sequences internal to the *SYN1* and/or glycoamidase transcriptional units. Experiments to define sequences required for the expression of *SYN1* are currently under way.

METHODS

Plant Material

Arabidopsis thaliana ecotype Wassilewskija was used in this study. Plants were grown on a commercial potting mix in a growth chamber at 20°C with a 16-hr-light and 8-hr-dark cycle. Approximately 15 to 18 days after germination, buds with lengths between 0.5 and 0.7 mm from prebolting plants were collected. Leaves were harvested from rosette-stage plants, whereas roots and seedlings were harvested from seeds sown on sterile agar plates. All samples were harvested, frozen in liquid N_2, and stored at −80°C until needed.

Confocal Microscopy

Anthers were fixed, squashed, and stained according to standard indirect immunofluorescence methods, incorporating the modifications of Peirson et al. (1997). After digestion with β-glucuronidase, cells were incubated overnight with 100 mg/mL mouse anti–β-tubulin antibody (Developmental Studies Hybridoma Bank, Johns Hopkins University, Baltimore, MD) in antibody buffer containing 0.05% Triton X-100. After buffer rinses, cells were treated for 6 hr with 10 mg/mL fluorescein isothiocyanate–conjugated, goat anti–mouse IgG (Jackson ImmunoResearch Laboratories Inc., West Grove, PA) in antibody dilution buffer containing 0.05% (v/v) Triton X-100. DNA was stained with 50 μg/mL propidium iodide in the presence of 10 mM Tris, pH 8.0, 10 mM NaCl, 0.1% Nonidet P-40, and 10 μg/mL RNase. Samples were viewed with a Nikon PCM-2000 confocal microscope system (Nikon Inc., Melville, NY). Z-sections were captured and stacked using Image Pro Plus software (Media Cybernetics, Silver Spring, MD).

Analysis of Prophase Chromosomes

Prophase chromosomes were analyzed essentially as described previously (Ross et al., 1996). Immature flower buds, ~0.5 mm, were harvested and fixed for 8 hr in ethanol–acetic acid (3:1) containing three drops per milliliter of a saturated ferric acetate solution in 50% acetic acid. After fixation, the buds were stored in 70% ethanol at 4°C until needed. Single buds were treated with 5 N HCL for 7 to 8 min and washed twice in distilled water, once in 50% ethanol, and two more times in distilled water. After removing the excess water, we broke the buds in a solution of 1% hematoxylin, 25% propionic acid, and 0.25% ferric ammonium sulfate (Henderson and Lu, 1968). The slide was carefully heated, and the preparation was gently squashed to spread the chromosomes. Slides were sealed and visualized using a Nikon Optiphot-2 microscope. The objective used in this study was a Nikon CFN Plan ×100 oil Achromat with iris; it had a numerical aperture of 1.25 to 0.5 and a 0.16-mm working distance. Images were captured on T-Max 400 film (Eastman Kodak).

Hybridizations

Genomic DNA was isolated from individual plants (Taylor et al., 1993). Approximately 10 μg of digested DNA was separated and transferred to nylon membranes by capillary transfer (Sambrook et al., 1989). Blots were hybridized in 0.5% nonfat dry milk, 1% SDS, and 4 × SSC (1 × SSC is 0.15 M NaCl and 0.015 M sodium citrate) at 55°C with probes that were labeled with α-^{32}P-dATP. After hybridization, blots were washed with 2 × SSC and 0.5% SDS, and radioactivity was detected using a PhosphorImager (Molecular Dynamics, Sunnyvale, CA).

Total RNA was isolated according to Verwoerd et al. (1989). Poly(A) RNA was isolated using oligo(dT) cellulose (Jacobson, 1987). Total RNA (20 μg) or poly(A) RNA (3 μg) was separated on 1% agarose gels containing 6% formaldehyde and 1 × Mops. After electrophoresis, the RNA was transferred to GeneScreen membranes (NEN Life Science Products, Boston, MA) (Sambrook et al., 1989), cross-linked, and prehybridized in 5% dextran sulfate, 1% SDS, and 1 M NaCl. Hybridization with radioactive probes, made by random priming, was conducted overnight at 60°C. After hybridization, blots were washed and viewed as described above.

Cloning the *SYN1* Gene

Plant DNA flanking the left border of the T-DNA insert was isolated by plasmid rescue (Behringer and Medford, 1992). DNA (10 μg) from a T_5 population that was segregating for *syn1* was digested with SalI, phenol extracted, and self-ligated in a total volume of 500 μL. The DNA was ethanol precipitated, resuspended in 10 μL of water, and

transformed into *Escherichia coli* DH10B cells. Ampicillin-resistant colonies were picked and screened by colony hybridization (Sambrook et al., 1989), using an α-^{32}P-dATP–labeled T-DNA left border as a probe. One class of clones containing both T-DNA left border and plant DNA was obtained. Restriction mapping indicated that the clone contained ~7.0 kb of plant DNA, which when used as a probe in DNA gel blot experiments hybridized with the expected fragments in *syn1* plants.

Wild-type DNA corresponding to the T-DNA insertion site in *syn1* plants was isolated from an Arabidopsis, ecotype Columbia, genomic library constructed in λ GEM (gift of E. Meyerowitz, California Institute of Technology, Pasadena, CA) by using the rescued plant DNA as a probe. Positive clones were isolated and characterized by restriction mapping and DNA gel blot analysis. One clone, λ syn1, which contained ~15 kb of DNA, was chosen for further characterization.

Subclones from λ syn1 were used to screen the PRL-2 cDNA library (a gift from C. Somerville, Carnegie Institute of Washington, Stanford, CA). Twenty clones, all containing similar 900-bp inserts, were obtained, which mapped to the 3′ end of the λ syn1 clone and correspond to a proline-rich protein-related gene. No cDNA clones corresponding to *SYN1* or the glycoamidase-like protein were obtained.

Genomic clones were subcloned into pBluescript SK+ (Stratagene, La Jolla, CA). Sequencing clones were generated by exonuclease III deletion (Henikoff, 1984) or direct subcloning (Sambrook et al., 1989). Dideoxy sequencing was performed using ^{35}S-dATP and a Sequenase quick denature plasmid sequencing kit (Amersham Life Sciences, Arlington Heights, IL). All regions of a 7.5-kb region were sequenced on both strands at least one time. Contigs and restriction maps were generated using DNASTAR programs (DNASTAR Inc., Madison, WI). Potential exons in the genomic DNA were identified by NetPlantGene version 1.0b (Hebsaard et al., 1996). BLAST searches were done to identify homologous sequences in the GenBank database (Altschul et al., 1990).

Isolation of the *SYN1* cDNA

The *SYN1* cDNA was isolated in a series of reverse transcription–polymerase chain reaction (RT-PCR) experiments. Primers corresponding to exon sequences predicted by NetPlantGene were used for reverse transcription and subsequent PCR amplification experiments. All reverse transcription experiments (Frohman et al., 1988) were conducted on poly(A) RNA that was purified from prebolting buds (5 mm). Exons A and 1 through 7 were cloned using primers BP2 and BF67 on cDNA that was generated by reverse transcription using primer BP8. Exons B and 1 through 7 were cloned using primers BP5 and BF67 on the same reverse-transcribed material. Exons 7 through 9 were cloned using primers XB1 and BP6 on cDNA generated via reverse transcription with primer BP8. Exons 9 through 13 were cloned using primers BF34 and BP7 on a cDNA template that was generated via reverse transcription by using primer XB8. Exons 12 through 18 and 17 through 20 were cloned by RT-PCR on cDNA that was reverse transcribed by using an oligo (dT) adapter primer with primers XB5 and XB8 and primers PA1 and PA3, respectively.

Experiments used to map the 5′ and 3′ ends of the cDNA included 5′ and 3′ rapid amplification of cDNA ends (RACE), according to the manufacturer's directions (as given in the user's manual published by Gibco BRL, Gaithersburg, MD), and inverse PCR (IPCR) (Huang, 1997). The 5′ terminus of the BP5 transcript was cloned by IPCR on cDNA generated by reverse transcription with either BP4 or BP6. After second strand synthesis and self-ligation, two rounds of PCR were conducted with primer set BP7 and BF67 followed by BP7 and XB4. The PCR products of BP7 and XB4 were blunt-end cloned into pBluescript SK+ at the SmaI site. Twelve clones were sequenced.

IPCR experiments were conducted for the BP2 transcript on cDNA generated by reverse transcription with either BP4 or BP6 by using primer XB7, which is specific for the BP2 transcript in exon A, and primer BP7. Final products of PCR amplification reactions with BP7 and XB7 were cloned into a T/A vector. Fifteen clones were sequenced.

ACKNOWLEDGMENTS

Many thanks to Ken Feldmann for providing access to the T-DNA mutant collection, Chris Somerville for providing the PRL-2 cDNA library, and Elliot Meyerowitz for providing the λ genomic DNA library. The mouse anti–β-tubulin used in this work was obtained from the Developmental Studies Hybridoma Bank maintained by the Department of Biology at the University of Iowa (Iowa City, IA). We are grateful for resources provided by the Electron Microscopy Facility at Miami University and Richard Edelmann for help with image analyses. Thanks also to Dawn Paxson-Sowders for critical reading of the manuscript. This research was supported by the U.S. Department of Agriculture (Grant No. 95-37304-2246).

Received October 1, 1998; accepted January 11, 1999.

REFERENCES

Albini, S., and Jones, G. (1987). Synaptonemal complex spreading in *Allium cepa* and *Allium fistulosum.* I. The initiation and sequence of pairing. Chromosoma **95,** 324–338.

Altschul, S., Gish, W., Miller, W., Myers, E., and Lipman, D. (1990). Basic local alignment search tool. J. Mol. Biol. **215,** 403–410.

An, Y., McDowell, J., Huang, S., McKinney, E., Chambliss, S., and Meagher, R. (1996). Strong, constitutive expression of the *Arabidopsis* ACT2/ACT8 actin subclass in vegetative tissues. Plant J. **10,** 107–121.

Anderson, L.K., Offenberg, H.H., Verkuijlen, W.M.H.C., and Heyting, C. (1997). RecA-like proteins are components of early meiotic nodules in lily. Proc. Natl. Acad. Sci. USA **94,** 6868–6873.

Beadle, G.W. (1932). Genes in maize for pollen sterility. Genetics **17,** 413–431.

Behringer, F.J., and Medford, J.I. (1992). A plasmid rescue technique for the recovery of plant DNA disrupted by T-DNA insertion. Plant Mol. Biol. Rep. **10,** 190–198.

Birkenbihl, R.P., and Subramani, S. (1992). Cloning and characterization of *rad21* an essential gene of *Schizosaccharomyces pombe* involved in double-strand-break repair. Nucleic Acids Res. **20,** 6605–6611.

Bishop, D.K. (1994). RecA homologs Dmc1 and Rad51 interact to form multiple nuclear complexes prior to meiotic chromosome synapsis. Cell **79,** 1081–1101.

Bishop, D.K., Park, D., Xu, L., and Kleckner, N. (1992). DMC1: A meiosis-specific yeast homolog of *E. coli* RecA required for recombination, synaptonemal complex formation and cell cycle progression. Cell **69,** 439–456.

Chaudhury, A.M., Lavithis, M., Taylor, P.E., Craig, S., Singh, M.B., Signer, E.R., Knox, R.B., and Dennis, E.S. (1994). Genetic control of male fertility in *Arabidopsis thaliana*: Structural analysis of premeiotic developmental mutants. Sex. Plant Reprod. **7,** 17–28.

Dawe, R.K. (1998). Meiotic chromosome organization and segregation in plants. Annu. Rev. Plant Physiol. Plant Mol. Biol. **49,** 371–395.

Dawson, J., Wilson, Z.A., Aarts, M.G.M., Braithwaite, A.F., Briarty, L.G., and Mulligan, B.J. (1993). Microspore and pollen development in six male-sterile mutants of *Arabidopsis thaliana.* Can. J. Bot. **71,** 629–638.

Frohman, M.A., Dush, M.K., and Martin, G.R., (1988). Rapid production of full-length cDNAs from rare transcripts: Amplification using a single gene-specific oligonucleotide. Proc. Natl. Acad. Sci. USA **85,** 8998–9002.

Ftouhi-Paquin, N., Hauers, C.R., Stack, R., Tarentino, A.L., and Plummer, T. (1997). Molecular cloning, primary structure, and properties of a new glycoamidase from the fungus *Aspergillus tubigensis.* J. Biol. Chem. **272,** 22960–22965.

Glover, J., Grelon, M., Craig, S., Chaudhury, A., and Dennis, E. (1998). Cloning and characterization of MS5 from Arabidopsis: A gene critical in male meiosis. Plant J. **15,** 345–356.

Golubovskaya, I.N., and Mashenkov, A.S. (1975). Genetic control of meiosis. I. Meiotic mutation in maize (*Zea mays* L.) *afd*, causing the elimination of the first meiotic division. Soviet Genet. **11,** 810–816.

Golubovskaya, I., Grebennikova, Z.K., Avalkina, N.A., and Sheridan, W.F. (1993). The role of the ameiotic gene in the initiation of meiosis and in the subsequent meiotic events in maize. Genetics **135,** 1151–1166.

Golubovskaya, I.N., Grebennikova, Z.K., Auger, D.L., and Sheridan, W.F. (1997). The maize desynaptic1 mutation disrupts meiotic chromosome synapsis. Dev. Genet. **21,** 146–159.

Green, I., and Sargan, D. (1991). Sequence of the cDNA encoding ovine tumor necrosis factor α: Problems with cloning by inverse PCR. Gene **109,** 203–210.

Guacci, V., Koshland, D., and Strunnikov, A. (1997). A direct link between sister chromatid cohesion and chromosome condensation revealed through the analysis of MCD1 in *S. cerevisiae.* Cell **91,** 47–57.

Hawley, R.S., and Arbel, T. (1993). Yeast meiosis and the fall of the classical view of meiosis. Cell **72,** 301–303.

He, C.P., Tirlapur, U., Cresti, M., Peja, M., Crone, D.E., and Mascarenhas, J.P. (1996). An *Arabidopsis* mutant showing aberrations in male meiosis. Sex. Plant Reprod. **9,** 54–57.

Hebsgaard, S.M., Korning, P.G., Tolstrup, N., Engelbrecht, J., Rouze, P., and Brunak, S. (1996). Splice site prediction in *Arabidopsis thaliana* DNA by combining local and global sequence information. Nucleic Acids Res. **24,** 3439–3452.

Henderson, S.A., and Lu, B.C. (1968). The use of haematoxylin for squash preparations of chromosomes. Stain Technol. **43,** 233–236.

Henikoff, S. (1984). Unidirectional digestion with exonuclease III creates targeted breakpoints for DNA sequencing. Gene **28,** 351–359.

Heo, S.-J., Tatebayashi, K., Kato, J., and Ikeda, H. (1998). The *RHC21* gene of budding yeast, a homologue of the fission yeast *rad21* gene, is essential for chromosome segregation. Mol. Gen. Genet. **257,** 149–156.

Higgins, D.G., and Sharp, P.M. (1989). Fast and sensitive multiple sequence alignments on a microcomputer. Comput. Appl. Biosci. **5,** 151–153.

Horton, P., and Nakai, K. (1996). A probabilistic classification system for predicting the cellular localization sites of proteins. Intellig. Syst. Mol. Biol. **4,** 109–115.

Huang, S.-H. (1997). Inverse PCR: An efficient approach to cloning cDNA ends. In Methods in Molecular Biology: PCR Cloning Protocols: From Molecular Cloning to Genetic Engineering, B.A. White, ed (New York: Humana Press), pp. 287–294.

Jacobson, A. (1987). Purification and fractionation of poly(A)$^+$ RNA. Methods Enzymol. **152,** 254–261.

Ji, L.-H., and Langridge, P. (1994). An early meiosis cDNA clone from wheat. Mol. Gen. Genet. **243,** 17–23.

Kitada, K., and Omura, T. (1983). Genetic control of meiosis in rice *Oryza sativa* L. II. Cytogenetical analyses of desynaptic mutants. Jpn. J. Genet. **58,** 567–577.

Kitada, K., and Omura, T. (1984). Genetic control of meiosis in rice, *Oryza sativa* L. IV. Cytogenetical analyses of asynaptic mutants. Can. J. Genet. Cytol. **26,** 264–271.

Kleckner, N. (1996). Meiosis: How could it work? Proc. Natl. Acad. Sci. USA **93,** 8167–8174.

Klimyuk, V.I., and Jones, J.D.G. (1997). *AtDMC1*, the *Arabidopsis* homologue of the yeast *DMC1* gene: Characterization, transposon-induced allelic variation and meiosis-associated expression. Plant J. **11,** 1–14.

Kobayashi, T., Kobayashi, E., Sato, S., Hotta, Y., Miyajima, N., Tanaka, A., and Tabata, S. (1994). Characterization of cDNAs induced in meiotic prophase in lily microspores. DNA Res. **1,** 15–26.

Lin, Y., Larson, K., Doer, R., and Smith, G. (1992). Meiotically induced *rec7* and *rec8* genes of *Schizosaccharomyces pombe.* Genetics **132,** 75–85.

Losada, A., Hirano, M., and Hirano, T. (1998). Identification of *Xenopus* SMC protein complexes required for sister chromatid cohesion. Genes Dev. **12,** 1986–1997.

Maguire, M., Riess, R., and Paredes, A. (1993). Evidence from a maize desynaptic mutant points to a probable role of synaptonemal complex central region components in provision for subsequent chiasma maintenance. Genome **36,** 797–807.

McKay, M.J., Troelstra, C., van der Spek, P., Kanaar, R., Smit, B., Hagemeijer, A., Bootsma, D., and Hoeijmakers, J. (1996). Sequence conservation of the *rad21 Schizosaccharomyces pombe* DNA double-strand break repair gene in human and mouse. Genomics **36,** 305–315.

Michaelis, C., Ciosk, R., and Nasmyth, K. (1997). Cohesins: Chromosomal proteins that prevent premature separation of sister chromatids. Cell **91,** 35–45.

Miyazaki, W.Y., and Orr-Weaver, T.L. (1994). Sister-chromatid cohesion in mitosis and meiosis. Annu. Rev. Genet. **28,** 167–187.

Moens, P. (1969). Genetic and cytological effects of three desynaptic genes in the tomato. Can. J. Genet. Cytol. **11,** 857–869.

Molnar, M., Bahler, J., Sipiczki, M., and Kohli, J. (1995). The *rec8* gene of *Schizosaccharomyces pombe* is involved in linear element formation, chromosome pairing and sister-chromatid cohesion during meiosis. Genetics **141,** 61–73.

Ogawa, H. (1993). RecA-like recombination proteins in eukaryotes: Functions and structures of *Rad51* genes. Cold Spring Harbor Symp. Quant. Biol. **58,** 569–576.

Orr-Weaver, T.L. (1995). Meiosis in *Drosophila*: Seeing is believing. Proc. Natl. Acad. Sci. USA **92,** 10443–10449.

Peirson, B.N., Owen, H.A., Feldmann, K.A., and Makaroff, C.A. (1996). Characterization of three male-sterile mutants of *Arabidopsis thaliana* exhibiting alterations in meiosis. Sex. Plant Reprod. **9,** 1–16.

Peirson, B.N., Bowling, S.E., and Makaroff, C.A. (1997). A defect in synapsis causes male sterility in a T-DNA–tagged *Arabidopsis thaliana* mutant. Plant J. **11,** 659–669.

Rechsteiner, M., and Rogers, S. (1996). PEST sequences and regulation by proteolysis. Trends Biol. Sci. **21,** 267–271.

Roeder, G.S. (1995). Sex and the single cell: Meiosis in yeast. Proc. Natl. Acad. Sci. USA **92,** 10450–10456.

Ross, K.J., Fransz, P., and Jones, G.H. (1996). A light microscopic atlas of meiosis in *Arabidopsis thaliana.* Chrom. Res. **4,** 507–516.

Ross, K.J., Fransz, P., Armstrong, S.J., Vizir, I., Mulligan, B., Franklin, F.C.H., and Jones, G.H. (1997). Cytological characterization of four meiotic mutants of *Arabidopsis* isolated from T-DNA–transformed lines. Chrom. Res. **5,** 551–559.

Sambrook, J., Fritsch, E.F., and Maniatis, T. (1989). Molecular Cloning: A Laboratory Manual, 2nd ed. (Cold Spring Harbor, NY: Cold Spring Harbor Laboratory Press).

Sato, S., Hotta, Y., and Tabata, S. (1995). Structural analysis of a *Rec-A* like gene in the genome of *Arabidopsis thaliana.* Chrom. Res. **2,** 89–93.

Sieburth, L.E., and Meyerowitz, E.M. (1997). Molecular dissection of the *AGAMOUS* control region shows that *cis* elements for spatial regulation are located intragenically. Plant Cell **9,** 355–365.

Singh, R.J. (1993). Genetic control of meiosis. In Plant Cytogenetics (Boca Raton, FL: CRC Press), pp. 39–62.

Spielman, M., Preuss, D., Li, F.L., Browne, W.E., Scott, R.J., and Dickinson, H.G. (1997). TETRASPORE is required for male meiotic cytokinesis in *Arabidopsis thaliana.* Development **124,** 2645–2657.

Stack, S.M., Sherman, J.D., Anderson, L.K., and Herickhoff, L.S. (1993). Meiotic nodules in vascular plants. Chrom. Today **11,** 301–311.

Staiger, C.J., and Cande, W.Z. (1993). Cytoskeletal analysis of maize meiotic mutants. In Molecular and Cell Biology of the Plant Cell Cycle, J.C. Ormrod and D. Francis, eds (Dordrecht, The Netherlands: Kluwer Academic Publishers), pp. 157–171.

Taylor, B.H., Manhart, J.R., and Amasino, R.M. (1993). Isolation and characterization of plant DNAs. In Methods in Plant Molecular Biology and Biotechnology, B.E Glick and J.R. Thompson, eds (Boca Raton, FL: CRC Press), pp. 37–41.

Terasawa, M., Shinohara, A., Hotta, Y., Ogawa, H., and Ogawa, T. (1995). Localization of RecA-like recombination proteins on chromosomes of the lily at various meiotic stages. Genes Dev. **9,** 925–934.

Verwoerd, T., Dekker, B., and Hoekema, A. (1989). A small-scale procedure for the rapid isolation of plant RNAs. Nucleic Acids Res. **17,** 2362.

Yu, S., Ozawa, M., Naved, A.F., Miyauchi, T., Muramatsu, H., and Muramatsu, T. (1995). cDNA cloning and sequence analysis of a novel calcium binding protein with oligoproline motif. Cell Struct. Funct. **20,** 263–268.

Zetka, M., and Rose, A. (1995). The genetics of meiosis in *Caenorhabditis elegans.* Trends Genet. **11,** 27–31.